Modeling of an ultrahigh-frequency resonator based on the relative vibrations of carbon nanotubes

Elena Bichoutskaia,[1,*] Andrei M. Popov,[2] Yurij E. Lozovik,[2] Olga V. Ershova,[3] Irina V. Lebedeva,[3,4,5] and Andrei A. Knizhnik[4,5]

[1]*Department of Chemistry, University of Nottingham, University Park, Nottingham NG7 2RD, United Kingdom*
[2]*Institute of Spectroscopy, Russian Academy of Sciences, Troitsk, 142190 Moscow Region, Russia*
[3]*Moscow Institute of Physics and Technology, Dolgoprudny, 141700 Moscow Region, Russia*
[4]*RRC "Kurchatov Institute," Kurchatov Sq. 1, 123182 Moscow, Russia*
[5]*Kinech Laboratory Ltd., Kurchatov Sq. 1, 123182 Moscow, Russia*

An ultrahigh frequency resonator based on the relative vibrations of the walls of carbon nanotubes is proposed and studied theoretically. Density functional theory is used to compute the energy of interaction of the walls as a function of their relative rotation and displacement along the principal axis of nanotube. The computed energy curves are fitted analytically and further exploited in the calculations of the frequencies of small relative axial and rotational vibrations of the walls. For a model resonator based on the (9,0)@(18,0) double-walled carbon nanotube with the movable outer wall, the microcanonical molecular dynamics simulations are performed to predict the quality factor of the resonance. Possible applications of the resonator are suggested, which include nanoscale mass detection. The estimated mass sensitivity of the proposed system reaches the atomic-mass limit at liquid-helium temperature.

I. INTRODUCTION

Active research in advanced functional materials is largely driven by a search of new concepts of nanodevices with potential technological and medical applications. Nano-electromechanical systems (NEMS) have a particular promise to radically change fundamental measurements at the molecular scale. Mechanical nanoresonators with the mass in the range of hundreds of femtograms and the operational frequencies in the region of 100 MHz to 1 GHz have been fabricated.[1–7] Due to small effective mass of their vibrating parts and small moment of inertia, nanoresonators can serve as very sensitive mass detectors capable of resolution in the range of $10^{-18}-10^{-21}$ g.[6–9] They have been used to weigh single bacteria[8] and detect single spins in magnetic-resonance systems enabling a wide variety of quantum-measurement experiments.[10]

Typically, nanoscale resonators are made from silicon. However, carbon nanotubes (CNTs) provide an alternative building material due to their unique atomic structure, high Young's modulus and low density. A significant progress has been made in constructing resonators based on the transverse vibrations of CNTs, which allow achieving the resonance frequency of 1.4 GHz.[6] If even higher resonance frequencies in CNTs were achieved, it would allow investigating the problems of fundamental interest such as the mechanisms of energy dissipation during ultrahigh frequency vibrations, as well as to continue the search for suitable CNTs-based mass sensors. However, realization of ultrahigh frequency resonators represents a significant experimental challenge. In cantilever CNTs, to reach the frequencies exceeding 2 GHz would require the use of impractically short nanotubes, less than 10 nm in length. In this paper, it is shown that the resonant frequencies of the relative vibrations of the walls of CNTs could potentially reach hundreds of GHz and critically

they do not depend on the size of the resonator. The latter would be a major advantage over the existing systems described in Refs. 1–9.

Two types of mechanical motion largely used in nanomechanical resonators are flexural and torsional vibrations. Flexural resonators are typically designed as cantilevers [Fig. 1(a)] or doubly clamped beams, and an example of torsional oscillator is a paddle [Fig. 1(b)]. A schematic of a resonator utilizing relative vibrations of the walls of carbon nanotubes is shown in Fig. 1(c). Motional freedom of the walls of CNTs has been exploited in a variety of NEMS designs[11–17] including important advances in building rotational and sliding electromechanical nanomotors[18–20] and memory cells.[21] Modeling the operational characteristics of these devices requires not only understanding of the nature of the interaction between the walls in CNTs but crucially its quantitative description. Both the position and the relative oscillations of the walls in double-walled carbon nanotubes (DWNTs) can be defined precisely if the interwall interaction energy is known. Furthermore, the values for the barriers to the relative motion of the walls can be extracted from the interwall interaction energy surface. Thus quantifying the interwall interaction is the next important stage in the development of NEMS based on DWNTs. In this paper, the interwall inter-
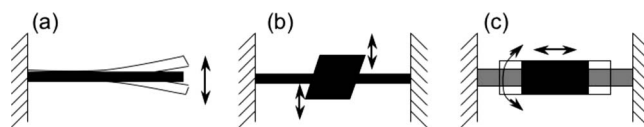

FIG. 1. Examples of nanoresonators based on mechanical vibrations: (a) a cantilever utilizing flexural vibrations (Ref. 5), (b) a paddle utilizing torsional vibrations (Ref. 75), (c) a resonator utilizing the relative vibrations of the walls of carbon nanotubes (this paper).

action energy as a function of the relative displacement and rotation of the walls is computed using density functional theory (DFT), fitted analytically and subsequently exploited in the calculations of the frequencies of the relative vibration of the walls. This provides a rigorous computational test for the quality of the obtained interwall interaction energy surfaces.

The paper is organized as follows. In Sec. II, small relative axial and rotational vibrations of the walls of CNTs are investigated theoretically. Section III presents the results of the microcanonical molecular dynamics (MD) simulations for the quality factor of an ultrahigh frequency nanoresonator based on the relative vibrations of DWNTs. Section IV is devoted to the discussion of possible applications for the proposed resonator with particular emphasis on mass detection. The conclusions are summarized in Sec. V.

II. INTERACTION AND VIBRATIONAL FREQUENCIES OF THE WALLS OF CARBON NANOTUBES

The relative vibrations of the walls of CNTs cause corrugations in the interwall interaction energy surface, which are orders of magnitude less than the average value of the interwall interaction energy. These corrugations are defined not only by the length of the interacting walls and the distance between the walls but also by their symmetry.[22,23] The interwall interaction in DWNTs has been studied extensively using a variety of computational methods.[23–32] For DWNTs with the interwall separation in the range of 3.4–3.7 Å, both DFT (Ref. 28) and tight-binding technique[29] calculations show that the radial displacements of the walls from coaxial position lead to significant increase in the interwall interaction energy. Therefore, the relative axial and rotational vibrations of the walls are not accompanied by the radial displacements, and the frequencies of these vibrations can be calculated using the dependence of the interwall interaction energy on the angle of the relative rotation of the walls, φ, and their relative displacement, z. Subsequently, the values for the barriers to the relative motion of the walls can be extracted from the $U(\varphi, z)$ surface.

According to semiempirical calculations,[25,32] for the $(n_1, n_1) @ (n_2, n_2)$ armchair and the $(n_1, 0) @ (n_2, 0)$ zigzag DWNTs the interwall interaction energy can be interpolated using the first harmonics of the Fourier expansion

$$U(\phi, z) = U_0 - U(\phi) - U(z)$$
$$= U_0 - \frac{\Delta U_\phi}{2}\cos\left(\frac{2\pi}{\delta_\phi}\phi\right) - \frac{\Delta U_z}{2}\cos\left(\frac{2\pi}{\delta_z}z\right), \quad (1)$$

where U_0 is the average interwall interaction energy, ΔU_ϕ and ΔU_z are the energy barriers to the relative rotation and sliding of the walls. In this paper, only the case of commensurate walls is considered for which U_0, ΔU_ϕ, and ΔU_z are proportional to the length of the overlap between the walls. Periods of the rotation and sliding between the equivalent positions are defined as $\delta_\phi = \frac{\pi N}{n_1 n_2}$ and $\delta_z = \frac{l_c}{2}$, where N is the greatest common factor of integers n_1 and n_2, and l_c is the length of the unit cell of DWNT. For DWNTs with compatible rotational symmetry of the walls $(N = n_1)$, the energy

barrier to the relative rotation, ΔU_ϕ, can be significant. For DWNTs with incompatible rotational symmetry of the walls $(N = 1)$, both *ab initio*[24] and semiempirical[25] results show that the dependence of the interwall interaction energy on the angle φ is typically very small so that the second term in expansion (1) can be neglected.

To test the adequacy of expansion (1) with density functional theory, the DFT AIMPRO code[33] with Perdew-Wang exchange-correlation functional[34] has been used. Integration over the Brillouin zone is approximated using the Monkhorst-Pack method[35] with 18 k-points sampling for DWNTs with armchair walls and 15 k-points sampling for DWNTs with zigzag walls. Basis set for carbon atom comprises the nonlocal norm-conserving core pseudopotential[36] extended with 38 Gaussian-type valence basis functions optimized for graphite structure. This approach predicts the interlayer binding energy in graphite of 35 meV/atom,[37] which is in good agreement with the experimental value.[38] Additionally, it reproduces the properties highly sensitive to the interlayer interaction, such as elastic and electronic properties of graphite. For example, the local density approximation (LDA) DFT C_{44} elastic constant for basal shear is computed to be 4.20 GPa,[37] whereas experiment[39] gives 5.05 ± 0.35 GPa.

The interwall interaction energies and the binding between the walls in carbon nanotubes, both nested and in bundles, have been previously studied using DFT,[24,26,28] and most recently including dispersion corrections.[40] However, these calculations did not clarify the importance of the dispersion interactions in the evaluation of the barriers to the rotation and sliding of the walls of carbon nanotubes with respect to one another. A recent study of the interaction of polycyclic aromatic hydrocarbons (PAHs) with graphene[41] showed that the dispersion interactions, although being most important contribution to the binding of these weakly bound systems, do not change the shape of the interaction energy surfaces or the value of the barriers to the motion of PAHs on graphene. These results underpin modeling using DFT of electromechanical devices based on the relative vibrations of graphene layers and telescoping carbon nanotubes.

The interwall interaction energies of the armchair $(6,6) @ (11,11)$ and the zigzag $(9,0) @ (18,0)$ DWNTs have been computed at a fixed angle ϕ and for five different values of the wall displacement z, including critical points of the surface such as global extrema and saddle points. The calculated DFT values and interpolation curves presented in Fig. 2 confirm that the interwall interaction energy of DWNTs can be satisfactorily interpolated using only first harmonics of the Fourier expansion (1). The average interwall interaction energy and the barriers to the relative motion of the walls are normalized per atom of the outer wall.

With the exception of Ref. 29 where the modes of rotational vibrations of a $(5,5) @ (10,10)$ DWNT were calculated, only the frequencies of the modes originating from vibrations of individual walls of DWNTs have been so far reported in the literature.[42–45] To calculate the frequencies of the relative vibrations of the walls, the second and third terms in expansion (1) of the interwall interaction energy surface are interpolated near the minimum using the harmonic potential as follows:
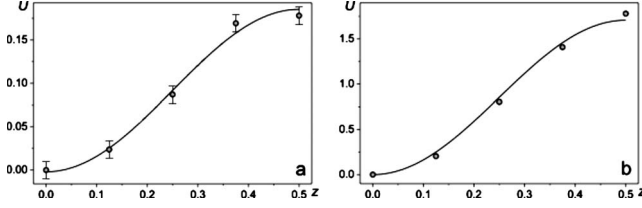
FIG. 2. The interwall interaction energy (in meV per atom of the outer wall) as a function of the wall displacement. (a): the (6,6)@(11,11) DWNT and (b): the (9,0)@(18,0) DWNT. The displacement z has the dimensionality of a fraction of a period of the relative sliding of the walls (δ_z). Circles show the calculated values of the energy and the solid line is interpolation of the energy using expansion (1). The energy minimum is positioned at $U=0$ and $z=0$.

$$U(z) = \frac{1}{2}k_z z^2, \quad U(\phi) = \frac{1}{2}k_\phi \phi^2 \qquad (2)$$

where

$$k_z = \frac{8n_2 l_{ov}\Delta U_z}{l_c}\left(\frac{2\pi}{l_c}\right)^2, \quad k_\phi = \frac{8n_2 l_{ov}\Delta U_\phi}{l_c}\left(\frac{n_1 n_2}{N}\right)^2. \qquad (3)$$

The frequencies ν_z and ν_ϕ of the axial and rotational vibrations of the walls can be determined as

$$\nu_z = \frac{1}{2\pi}\sqrt{\frac{k_z}{M}}, \quad \nu_\phi = \frac{1}{2\pi}\sqrt{\frac{k_\phi}{J}}, \qquad (4)$$

where M is the reduced mass and J is the reduced moment of inertia of the two walls.

If only the inner wall of DWNT, denoted as 1, is moving its moment of inertia and the mass can be expressed as

$$J_1 = M_1 R_1^2, \quad M_1 = \frac{4n_1 m_C l_1}{l_c}, \qquad (5)$$

where m_C is the mass of carbon atom. Similarly, if only the outer wall 2 is moving then

$$J_2 = M_2 R_2^2, \quad M_2 = \frac{4n_2 m_C l_2}{l_c}. \qquad (6)$$

Finally, the reduced moment of inertia and the reduced mass of both moving walls are defined as

$$J_{12} = \frac{J_1 J_2}{J_1 + J_2}, \quad M_{12} = \frac{M_1 M_2}{M_1 + M_2}. \qquad (7)$$

In the latter case, the reduced mass and the reduced moment of inertia imply that DWNT is not fixed between the electrodes but floating without friction. Although DWNTs with both walls moving cannot be realized in the laboratory conditions, it is not at all impossible as fullerenes and multi-shelled carbon nanoparticles were observed in the interstellar medium.[46] Thus, a possibility of the presence of CNTs in the interstellar medium or future studies of CNTs in a space laboratory should not be neglected.

The frequencies of the axial and rotational vibrations do not depend on the length of DWNT if both walls have the same length or if the longer wall is fixed and not moving. In

TABLE I. The frequencies (in GHz) of vibrations of the walls of DWNTs: $v_{z,1}$ are $v_{z,2}$ the frequencies of vibrations of the inner and outer wall, correspondingly, and $v_{z,12}$ is the frequency of the relative axial vibrations of both walls.

DWNT	$v_{z,1}$	$v_{z,2}$	$v_{z,12}$
(4,4)@(10,10)	108 ± 22	68 ± 14	128 ± 26
(5,5)@(11,11)	121 ± 15	81 ± 10	146 ± 18
(6,6)@(12,12)	129 ± 13	91 ± 9	158 ± 15
(5,5)@(10,10)	277 ± 7	196 ± 5	340 ± 8
(6,6)@(11,11)	304 ± 8	224 ± 6	380 ± 10
(7,7)@(12,12)	319 ± 4	243 ± 3	401 ± 5
(9,0)@(18,0)	577 ± 1	397.4 ± 0.5	701 ± 1
(10,0)@(20,0)	312 ± 1	221 ± 1	382 ± 1

such cases, the length of the overlap between the walls is equal to the length of vibrating walls, i.e., $l_{ov} = l_1$ or (and) $l_{ov} = l_2$. Inserting expressions (3) for k_z and k_ϕ, into Eq. (4) together with the relevant expressions for M and J given above, the frequencies of the relative vibrations of the walls can be defined as follows:

$$\nu_{z,1} = \frac{1}{l_c}\sqrt{\frac{2n_2\Delta U_z}{n_1 m_C}}, \quad \nu_{z,2} = \frac{1}{l_c}\sqrt{\frac{2\Delta U_z}{m_C}},$$

$$\nu_{z,12} = \frac{1}{l_c}\sqrt{\frac{2(n_1 + n_2)\Delta U_z}{n_1 m_C}}, \qquad (8)$$

where $\nu_{z,1}$ and $\nu_{z,2}$ are the frequencies of the axial sliding vibrations of the inner and outer wall, correspondingly, and $\nu_{z,12}$ is the frequency of the relative axial sliding vibrations of the walls. Similarly, the frequencies $\nu_{\phi,1}$, $\nu_{\phi,2}$, and $\nu_{\phi,12}$ of the rotational vibrations of the walls are given by the following expressions:

$$\nu_{\phi,1} = \frac{n_2}{\pi N R_1}\sqrt{\frac{n_1 n_2 \Delta U_\phi}{2m_C}}, \quad \nu_{\phi,2} = \frac{n_1 n_2}{\pi N R_2}\sqrt{\frac{\Delta U_\phi}{2m_C}},$$

$$\nu_{\phi,12} = \frac{n_2}{\pi N R_1 R_2}\sqrt{\frac{n_1(n_1 R_1^2 + n_2 R_2^2)\Delta U_\phi}{2m_C}}. \qquad (9)$$

The frequencies of the axial sliding vibrations of the walls calculated for a set of DWNTs using expressions (8) are presented in Table I. It is interesting to note that the change in the frequencies is determined by the interplay between the change in the energy barrier to the relative sliding of the walls and the mass of the walls. For example, $\nu_{z,1}$ should go up with the increase in the energy barrier and the decrease in the mass of the inner wall 1. The DFT values for the energy barriers to the relative motion the walls are taken from Ref. 24 where it was shown that for the armchair $(n,n)@(n+5,n+5)$ and $(n,n)@(n+6,n+6)$ DWNTs the barrier to the relative sliding of the walls increases with the increase in the radius (and, hence, the mass) of nanotube. Table I shows that in this case, for a given outer wall, the frequency of the axial vibrations of the inner wall significantly increases even with the increase in the mass of the inner wall thus leading to the conclusion that the change in

the value of the energy barrier is the dominant effect. Although the values of the radii and interwall distances are very close in the armchair (5,5)@(10,10) DWNT and the zigzag (9,0)@(18,0) DWNT, the barrier to the relative sliding of the walls is an order of magnitude higher in the (9,0)@(18,0) DWNT.[24] This fact is reflected in the high values of the frequencies of vibrations of the walls of the (9,0)@(18,0) DWNT. For the (5,5)@(10,10) DWNT, frequencies of the rotational vibrations of the walls have been also estimated and the values are $\nu_{\phi,1}=530$ GHz, $\nu_{\phi,2}=190$ GHz, and $\nu_{\phi,12}=570$ GHz (the DFT values of the radii R_1 and R_2 are taken from Ref. 24). These values are smaller by a factor of 2 than the frequencies of the rotational vibrations calculated in Ref. 29. The discrepancy in the results is due to the fact that for the (5,5)@(10,10) DWNT the tight-binding method predicts greater value for the barrier to the relative rotation of the walls. The frequencies of the rotational vibrations of the walls of the (5,5)@(10,10) DWNT calculated in this paper are in a good agreement with the frequencies of the rotational vibrations in a bundle of (10,10) CNTs (Ref. 47) lying in the region of 300–360 GHz. For the (6,6)@(12,12), (9,0)@(18,0), and (10,0)@(20,0) DWNTs, the frequencies of the relative rotational vibrations are estimated to be in the range of 30–300 GHz. Note that these frequencies exceed by 2 orders of magnitude the currently achieved record of 1.4 GHz (Ref. 6) of the resonant frequencies in nanoresonators.

Equations (9) require data on the chirality indices and radii of the constituent walls. If the chirality indices were known, the radius of the wall could be estimated using approximate expression $R=a_0\alpha n/2\pi$, where a_0 is the carbon-carbon bond length in graphite, $\alpha=\sqrt{3}$ for the armchair (n,n) walls, and $\alpha=1$ for the $(n,0)$ zigzag walls. If the expression above is substituted into Eqs. (9), the frequencies of the rotational vibrations of the walls take the following form:

$$\nu_{\phi,1}=\frac{n_2}{N\alpha a_0}\sqrt{\frac{2n_2\Delta U_\phi}{n_1 m_C}}, \quad \nu_{\phi,2}=\frac{n_1}{N\alpha a_0}\sqrt{\frac{2\Delta U_\phi}{m_C}},$$

$$\nu_{\phi,12}=\frac{1}{N\alpha a_0}\sqrt{\frac{2(n_1^3+n_2^3)\Delta U_\phi}{n_1 m_C}}. \tag{10}$$

According to Ref. 48, vibrations of the walls of DWNTs along the principal axis are infrared active, whereas the rotational vibrations are Raman active. The calculated frequencies can be therefore measured using appropriate techniques of terahertz and Raman spectroscopy. In such measurements, the calculated frequencies should be distinguishable from the frequencies of the vibration modes of individual walls. Electron diffraction method has been suggested recently,[49] which allows examining the chirality indices of both the outer and the inner walls of an isolated DWNT. This method could be used to select DWNTs for experimental realization of the ultrahigh frequency resonator described in the next section and to study the relative motion of the walls of DWNTs.

III. ULTRAHIGH FREQUENCY RESONATOR: MOLECULAR DYNAMICS SIMULATIONS

The proposed ultrahigh frequency resonator comprises a DWNT with the long inner wall attached to the source and
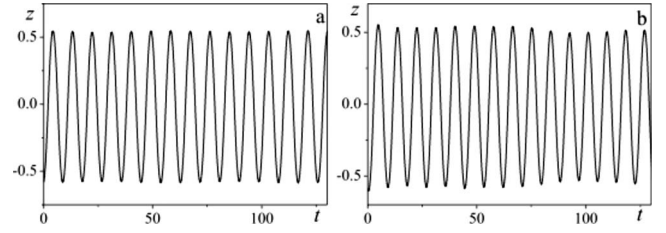

FIG. 3. The displacement (in Å) of the outer wall of the (9,0)@(18,0) DWNT as a function of time (in ps) at (a) $T=4.2$ K and (b) $T=77$ K.

the drain electrodes, and the short outer wall (shuttle) that can move along the inner wall between the source and the drain electrodes and/or about the nanotube axis. In principle, the resonator could be built from multiwalled carbon nanotubes, analogous to the design of recently realized nanotube-based motors.[18–20] The vibrations of the walls are excited by applying an alternating voltage between the source and the drain electrode at the frequency of resonance.

To estimate the quality factor of the resonance in the proposed system, the MD simulations of the resonator based on a (9,0)@(18,0) DWNT with the movable outer wall have been performed (see detailed methodology in Refs. 50 and 51). Van der Waals interaction between carbon atoms of the inner and the outer walls is described using the Lennard-Jones 12–6 potential $U=4\varepsilon[(\sigma/r)^{12}-(\sigma/r)^6]$ with parameters $\varepsilon=3.73$ meV and $\sigma=0.34$ nm taken from the AMBER database.[52] The cut-off distance of the Lennard-Jones potential is taken to be 2 nm. The covalent carbon-carbon interactions are described using the empirical Brenner potential,[53] which was shown to correctly reproduce vibrational spectra of both defected and defect-free carbon nanotubes.[54]

Periodic boundary conditions are applied along the principal axis of the DWNT. The length of the outer (18,0) wall is taken to be 2 nm, and the length of the simulation cell is 6.3 nm, sufficient to exclude the interactions between the shuttles in the neighboring cells. Small free oscillations of the outer wall along the principal axis of the DWNT are allowed with the initial amplitude of 0.58 Å. Ten simulations with different initial distributions of velocities of the atoms are performed at liquid-nitrogen temperature of 77 K and seven simulations are performed at liquid-helium temperature of 4.2 K. The duration of each simulation is between 100 and 130 ps. The time steps used are 0.1 and 0.3 fs at the temperature values of 4.2 and 77 K, respectively. In the latter case, the time step is two orders of magnitude smaller than the period of the thermal vibrations of carbon atoms. Typical examples of the dependence of the wall displacement on time presented in Fig. 3 show the damped oscillations of the outer wall. The average values of the Q factors obtained are $Q=160\pm80$ at 77 K and $Q=540\pm240$ at 4.2 K.

Since the energy loss per oscillation period and the thermal kinetic energy per degree of freedom are of the same order of magnitude, considerable thermodynamic fluctuations of the Q factor have been observed in the proposed model system. Furthermore, the Q factor averaged over one simulation is sensitive to the initial distribution of coordinates and velocities of carbon atoms. This explains a large

calculation error of the Q factor. The thermodynamic fluctuations can also impose restrictions on the minimum size of NEMS. This problem has been studied in Ref. 51 for a DWNT based gigahertz oscillator using MD simulations and theoretical analysis in the framework of the fluctuation-dissipation theorem. The computed values of the Q factors are in good general agreement with those typical for DWNT based NEMS. The Q factor values of the DWNT-based oscillators with large telescopic oscillations of the walls were first calculated in Ref. 51 as well as estimated from the data previously obtained in MD simulations,[55,56] and the Q values of 300–800 were predicted at very low temperatures of 0–8 K. These estimates also showed significant increase in the values of Q factor with the decrease in temperature. In cantilever resonators based on multiwalled nanotubes and ropes of CNTs, measurements yielded the Q values in the range of 150–2500 at room temperature.[10,57–62]

Typically, the dissipation mechanisms and the overall behavior of the loss in nanoresonators based on CNTs are very complicated and no single mechanism is dominant. The energy losses can be divided into two general categories: the intrinsic and extrinsic losses. The intrinsic losses, such as phonon-phonon and phonon-electron interactions, are fundamental "internal friction" processes within the lattice and can arise even in a perfect crystal. These dissipation mechanisms set the absolute limit to the performance of a mechanical resonator. Additional dissipation arises from imperfections of the lattice, such as defects, impurities, and dangling bonds. The extrinsic losses occur due to interactions with the surrounding media such as air friction, clamping, and measurement scheme. All the above losses will affect the performance and lower the Q factor of any nanoresonator based on CNTs.

To achieve greater Q factors in a resonator based on the relative vibrations of the walls of CNTs, the resonance between the frequencies of the modes originating from the vibrational modes of the individual walls and the frequencies of their relative axial or rotational vibrations should be avoided. For considered DWNTs with diameters less than 1.5 nm, the lowest frequency modes are the squeezing-like mode lying between 0.9 and 1.2 THz,[43] and the longitudinal and twisting modes, which occupy the region between 1.05 and 1.5 THz.[45] Therefore, the resonances are absent for resonators based on DWNTs with small diameters. The semiempirical[25] calculations show that the barrier to the relative sliding of the nonchiral walls goes up very weakly with the increase in the diameter of DWNT soon reaching a plateau. Therefore the frequencies of the relative vibrations of the walls, as given by Eqs. (8) and (9), also increase only slightly with the increase in the DWNT diameter. Using the results obtained in Ref. 25 the increase in the frequencies is estimated as 10% if the diameter goes up from 1.5 to 3 nm, and 20% if the diameter is increased from 1.5 to 10 nm. The frequencies of the longitudinal and twisting modes however do not depend on the DWNT diameter,[45] and the frequencies of vibrations of breathing-like modes[42] and squeezing-like modes[43] go down. For DWNTs with diameters greater than 3 nm, the frequencies of the relative vibrations of the walls along the axis and squeezing-like modes may lie in the same frequency range. When the diameter exceeds 10 nm,

breathing-like modes could also be found in this frequency region. Thus, high values of the Q factor are achievable in resonators based on DWNTs only with diameters less than 3 nm.

IV. POSSIBLE APPLICATIONS OF ULTRAHIGH FREQUENCY RESONATOR

The proposed design of the resonator provides an ideal platform for experimental study of fundamental physical processes in NEMS such as mechanisms of dissipation of kinetic energy, the interaction of the nanometer-scale objects, and the frequencies of their relative vibrations. Since the direct experimental measurements of the barriers to the relative motion of the walls are currently not available, the measurements of the frequencies of the vibrations of the walls would be an excellent experimental test for the quality of the energy surfaces. The proposed resonator also exhibits promise as a precise mass sensor.

Mass sensors operate by measuring the frequency shift of the resonance as additional mass, i.e., a molecule, a molecular cluster, or a nanoparticle, is adsorbed on the short shuttle of the proposed resonator. By measuring and comparing the resonant frequencies of the relative vibrations of the unloaded outer wall and the wall with cargo, the added mass of the nano-object could be determined. Using expression (4) for the resonant frequency of the oscillating wall, the sensitivities of mass and frequency measurements can be connected as follows:

$$\frac{\delta M}{M} = \frac{2\delta\nu_z}{\nu_z}, \tag{11}$$

where $\delta\nu_z$ is the line width of the resonant line.

The frequency resolution of nanoresonator is determined by various fundamental noise processes such as the thermomechanical noise originating from thermally driven motion of the device,[2,63–65] Nyquist-Johnson noise associated with the readout circuitry,[66] adsorption-desorption and momentum-exchange noises[2,65,67] resulting from the interaction with the residual gas molecules, and noise related to the temperature fluctuations due to a finite thermal conductance of the resonator.[2,65,68] However, the inherent resolution of nanoresonator is mainly related to the thermomechanical noise, which, for the measurement bandwidth $\Delta f \ll \nu_z/Q$, is given by the following expression:

$$\delta\nu_z \approx \nu_z\sqrt{\frac{k_B T}{E}}\sqrt{\frac{\Delta f}{2\pi Q\nu_z}}, \tag{12}$$

where k_B is Boltzmann's constant, T is the temperature, and E is the oscillation energy.[2] For $\Delta f > \nu_z/Q$, the upper limit of the frequency resolution can be estimated as

$$\delta\nu_z \leq \frac{\nu_z}{Q}\sqrt{\frac{k_B T}{2\pi E}}. \tag{13}$$

The measurement bandwidth Δf can reach 1 kHz–10 MHz.[2] Using expression (11) the upper estimate for the mass sensitivity related to the thermomechanical noise in nanoresonators can be obtained as follows:
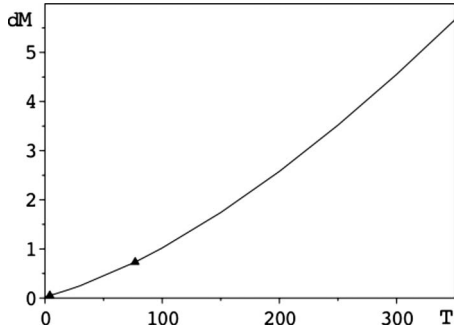
FIG. 4. The dependence of the upper limit of mass sensitivity δM (in m_C) of the proposed nanoresonator based on a (9,0)@(18,0) DWNT on the temperature T (in K). Triangles indicate the points for which the MD simulations were performed in this paper.

$$\delta M \leq \frac{2M}{Q}\sqrt{\frac{k_B T}{2\pi E}}. \tag{14}$$

In the proposed model resonator based on the (9,0)@(18,0) DWNT, the mass of the oscillating (18,0) wall equals to $360 m_C$, thus the mass sensitivity of the resonator can be estimated using formula (14) as $0.7 m_C$ for 77 K and $0.05 m_C$ for 4.2 K. An advantage of the design compared to the cantilever resonators is that the relation between shifts in the resonant frequency and changes in the mass depends only on the geometry of the resonator, and does not depend on the position of adsorbed particle. A nanomotor driven by a thermal gradient imposed along the device architecture has been produced in recent experiments of Barreiro,[20] in which a nano-object was attached to a short outer wall of a multiwalled carbon nanotube that could move along its inner core. The Barreiro motor could also be used to build a nanoresonator for the atomic-resolution mass measurements. For the experimental dimensions of the outer wall reported in Ref. [20] as 300 nm in length and 7 nm diameter, which approximately correspond to $n_2 \approx 90$ for the zigzag DWNT, the sensitivity of the Barreiro device estimated using Eq. (14) is $20 m_C$ for the quality factor of 160 and $1.4 m_C$ for the quality factor of 540.

Sensitivity of the resonator can be improved with decrease in the temperature as well as the length and diameter of the moving outer wall. Figure 4 shows the dependence of the upper limit of the mass sensitivity on the temperature calculated for the proposed resonator based on the (9,0)@(18,0) DWNT with the fixed length of the outer wall $L=2$ nm. If the amplitude of oscillations in the proposed resonator is constant, the oscillation energy E is proportional to the length L and the diameter D of the moving outer wall. Therefore, the mass sensitivity has a square-root dependence on L and D, as seen in Fig. 5. Figure 5 compares the dependencies of the mass sensitivity on L and D for the resonator based on a (9,0)@(18,0) DWNT with $D=1.4$ nm and the Barreiro motor with $D=7$ nm for two different values of Q factor, $Q=540$ and $Q=160$. We expect the Q factor of the proposed resonator to be inversely proportional to the temperature, similar to that of the gigahertz oscillator based on a carbon nanotube.[51]
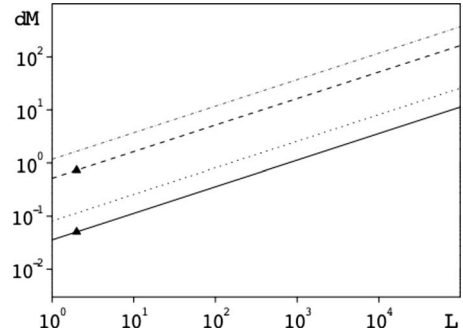

FIG. 5. The dependence of the upper limit of mass sensitivity δM (in m_C) of the proposed nanoresonator based on a (9,0)@(18,0) DWNT on the length of the moving outer wall L (in nm): $Q=540$, $D=1.4$ nm (solid line); $Q=160$, $D=1.4$ nm (dashed line); $Q=540$, $D=7$ nm (dotted line); and $Q=160$, $D=7$ nm (dash-dotted line). Triangles indicate the points for which the MD simulations were performed in this paper.

Inducing and detecting the relative vibrations of the CNTs walls with the amplitudes of subnanometer scale at extremely high resonant frequencies becomes a real challenge. Tunable narrow-band subterahertz radiation techniques have been developed very recently[69,70] and these could be used for inducing the relative vibrations of the walls of CNTs. The detection of tunnel current through the STM tip fixed near the surface of the vibrating wall may provide a way for experimental measurements of extremely small amplitudes of vibrations at very high frequencies. Measurements of the conductivity between the source and the drain electrode as a function of the applied frequency of subterahertz radiation could provide an alternative solution to the detection of the resonance frequency of CNTs. The conductivity of DWNT with a short outer wall depends significantly on the position of the outer wall and hence very sensitive to its vibrations.[13,71]

The large resistances of the small structures complicate all the detection methods that measure charge through small structures. At high resonance frequencies, such high resistances lead to a frequency-dependent signal attenuation due to a high RC time constant. There are two methods currently proposed to work around this problem. One is to transform the impedance of the measured device at the frequency of interest.[72] Another method is to use a nonlinear component in the circuit, such as piezoresistor, to perform downmixing at a much lower frequency, where the signal attenuation is not large.[73,74]

V. CONCLUSIONS

This study combines density functional theory and microcanonical molecular-dynamics simulations to model a type of ultrahigh frequency resonator based on the relative vibrations of the walls of carbon nanotubes. For a set of armchair and zigzag DWNTs, the energy of the interaction of the walls is computed as a function of their relative displacement and rotation using LDA-DFT with periodic boundary conditions and Gaussian-type orbitals. The obtained energy dependen-

cies are used to predict the frequencies of the small relative axial and rotational vibrations of the walls. The calculated frequencies lie in the range of 70–700 GHz. It has been shown that in the case of fixed long inner wall and moving short outer wall, the frequencies of their relative vibrations do not depend on the length of the walls.

The mass of a nano-object attached to the vibrating wall of the resonator can be determined by measuring the resonance frequency of the system. In the proposed design, the frequency depends only on the mass of the added nano-object and does not depend on the size of the resonator or on the position of the nano-object. To estimate the sensitivity of mass detection and the quality factor of the resonance, MD simulations of the model resonator based on a $(9,0)@(18,0)$ DWNT with the movable outer wall have been performed. The estimated average values of the Q factor of the model resonator are $Q=160$ at 77 K and $Q=540$ at 4.2 K with the mass sensitivity less than the mass of a single carbon atom.

Recent advances in techniques allowing determination of the chirality indices of both walls of an isolated DWNT,[49] realization of CNT-based nanomotors with a rotor made of the short outer sleeve and a stator made of the long inner core,[18–20] and the resonance frequency measurements in resonators based on the transverse vibrations of CNTs (Refs. 6–8 and 10) give us a cause for the optimism that the proposed nanoresonator will be soon produced using existing methods of modern nanotechnology.

*Corresponding author; elena.bichoutskaia@nottingham.ac.uk

[1] K. L. Ekinci, X. M. H. Huang, and M. L. Roukes, Appl. Phys. Lett. **84**, 4469 (2004).

[2] K. L. Ekinci, Y. T. Yang, and M. L. Roukes, J. Appl. Phys. **95**, 2682 (2004).

[3] Y. T. Yang, C. Callegari, X. L. Feng, K. L. Ekinci, and M. L. Roukes, Nano Lett. **6**, 583 (2006).

[4] X. L. Feng, R. R. He, P. D. Yang, and M. L. Roukes, Nano Lett. **7**, 1953 (2007).

[5] B. Ilic, H. G. Craighead, S. Krylov, W. Senaratne, and C. Ober, J. Appl. Phys. **95**, 3694 (2004).

[6] H. B. Peng, C. W. Chang, S. Aloni, T. D. Yuzvinsky, and A. Zettl, Phys. Rev. Lett. **97**, 087203 (2006).

[7] K. Jensen, K. Kwanpyo, and A. Zettl, Nat. Nanotechnol. **3**, 533 (2008).

[8] H. G. Craighead, Science **290**, 1532 (2000).

[9] D. Rugar, R. Budakian, H. J. Mamin, and B. W. Chui, Nature (London) **430**, 329 (2004).

[10] V. Sazonova, Y. Yaish, H. Ustunel, D. Roundy, T. A. Arias, and P. L. McEuen, Nature (London) **431**, 284 (2004).

[11] E. Bichoutskaia, Phil. Trans. R. Soc. London, Ser. A **365**, 2893 (2007).

[12] A. M. Popov, E. Bichoutskaia, Y. E. Lozovik, and A. S. Kulish, Phys. Status Solidi A **204**, 1911 (2007).

[13] E. Bichoutskaia, A. M. Popov, Y. E. Lozovik, G. S. Ivanchenko, and N. G. Lebedev, Phys. Lett. A **366**, 480 (2007).

[14] E. Bichoutskaia, A. M. Popov, M. I. Heggie, and Y. E. Lozovik, Fullerenes, Nanotubes, Carbon Nanostruct. **14**, 131 (2006).

[15] A. S. Kulish, A. M. Popov, Y. E. Lozovik, and E. Bichoutskaia, Fullerenes, Nanotubes, Carbon Nanostruct. **16**, 340 (2008).

[16] E. Bichoutskaia, A. M. Popov, and Y. E. Lozovik, Mater. Today **11**, 38 (2008).

[17] A. M. Popov, Y. E. Lozovik, E. Bichoutskaia, G. S. Ivanchenko, N. G. Lebedev, and E. K. Krivorotov, Fullerenes, Nanotubes, Carbon Nanostruct. **16**, 352 (2008).

[18] A. M. Fennimore, T. D. Yuzvinsky, W. Q. Han, M. S. Fuhrer, J. Cumings, and A. Zettl, Nature (London) **424**, 408 (2003).

[19] B. Bourlon, D. C. Glatti, L. Forro, and A. Bachtold, Nano Lett. **4**, 709 (2004).

[20] A. Barreiro, R. Rurali, E. R. Hernandez, J. Moser, T. Pichler, L. Forro, and A. Bachtold, Science **320**, 775 (2008).

[21] V. V. Deshpande, H.-Y. Chiu, Ch. H. W. Postma, C. Miko, L. Forro, and M. Bockrath, Nano Lett. **6**, 1092 (2006).

[22] M. Damnjanovic, I. Milosevic, T. Vukovic, and R. Sredanovic, Phys. Rev. B **60**, 2728 (1999).

[23] T. Vukovic, M. Damnjanovic, and I. Milosevic, Physica E (Amsterdam) **16**, 259 (2003).

[24] E. Bichoutskaia, M. I. Heggie, A. M. Popov, and Y. E. Lozovik, Phys. Rev. B **73**, 045435 (2006).

[25] A. V. Belikov, Y. E. Lozovik, A. G. Nikolaev, and A. M. Popov, Chem. Phys. Lett. **385**, 72 (2004).

[26] E. Bichoutskaia, A. M. Popov, A. El-Barbary, M. I. Heggie, and Y. E. Lozovik, Phys. Rev. B **71**, 113403 (2005).

[27] R. Saito, R. Matsuo, T. Kimura, G. Dresselhaus, and M. S. Dresselhaus, Chem. Phys. Lett. **348**, 187 (2001).

[28] J.-C. Charlier and J. P. Michenaud, Phys. Rev. Lett. **70**, 1858 (1993).

[29] Y. K. Kwon and D. Tomanek, Phys. Rev. B **58**, R16001 (1998).

[30] A. H. R. Palser, Phys. Chem. Chem. Phys. **1**, 4459 (1999).

[31] A. Szabados, L. P. Biro, and P. R. Surjan, Phys. Rev. B **73**, 195404 (2006).

[32] M. Damnjanovic, E. Dobardzic, I. Milosevic, T. Vukovic, and B. Nikolic, New J. Phys. **5**, 148 (2003).

[33] P. R. Briddon and R. Jones, Phys. Status Solidi **217**, 131 (2000).

[34] J. P. Perdew and Y. Wang, Phys. Rev. B **45**, 13244 (1992).

[35] H. J. Monkhorst and J. D. Pack, Phys. Rev. B **13**, 5188 (1976).

[36] G. B. Bachelet, D. R. Hamann, and M. Schluter, Phys. Rev. B **26**, 4199 (1982).

[37] R. H. Telling and M. I. Heggie, Philos. Mag. Lett. **83**, 411 (2003).

[38] L. X. Benedict, N. G. Chopra, M. L. Cohen, A. Zettl, S. G. Lonie, and V. H. Crespi, Chem. Phys. Lett. **286**, 490 (1998).

[39] C. S. G. Cousins and M. I. Heggie, Phys. Rev. B **67**, 024109 (2003).

[40] J. Kleis, E. Schroder, and P. Hyldgaard, Phys. Rev. B **77**, 205422 (2008).

[41] O. Ershova and E. Bichoutskaia, Phys. Chem. Chem. Phys. (to be published).

[42] V. N. Popov and L. Henrard, Phys. Rev. B **65**, 235415 (2002).

[43] T. Vukovic, S. Dmitrovic, and E. Dobardzic, Nanotechnology **17**, 747 (2006).

[44] R. Pfeiffer, F. Simon, H. Kuzmany, V. N. Popov, V. Zolyomi, and J. Kurti, Phys. Status Solidi B **243**, 3268 (2006).

[45] E. Dobardzic, I. Milosevic, T. Vukovic, B. Nikolic, and M. Damnjanovic, Eur. Phys. J. B **34**, 409 (2003).

[46] S. Iglesias-Groth, Astrophys. J. **608**, L37 (2004).

[47] Y. K. Kwon, S. Saito, and D. Tomanek, Phys. Rev. B **58**, R13314 (1998).

[48] G. S. Ivanchenko and N. G. Lebedev, Phys. Solid State **48**, 2354 (2006).

[49] K. Hirahara, M. Kociak, S. Bandow, T. Nakahira, K. Itoh, Y. Saito, and S. Iijima, Phys. Rev. B **73**, 195420 (2006).

[50] O. V. Ershova, Yu E. Lozovik, A. M. Popov, O. N. Bubel', E. F. Kislyakov, N. A. Poklonskii, A. A. Knizhnik, and I. V. Lebedeva, JETP **107**, 653 (2008).

[51] I. V. Lebedeva, A. A. Knizhnik, A. M. Popov, Yu E. Lozovik, and B. V. Potapkin, Nanotechnology **20**, 105202 (2009).

[52] http://amber.scripps.edu

[53] D. W. Brenner, O. A. Shenderova, J. A. Harrison, S. J. Stuart, B. Ni, and S. B. Sinnott, J. Phys.: Condens. Matter **14**, 783 (2002).

[54] M. Vandescuren, H. Amara, R. Langlet, and P. Lambin, Carbon **45**, 349 (2007).

[55] C.-C. Ma, Y. Zhao, Y.-C. Yam, G. Chen, and Q. Jiang, Nanotechnology **16**, 1253 (2005).

[56] W. Guo, Y. Guo, H. Gao, Q. Zheng, and W. Zhong, Phys. Rev. Lett. **91**, 125501 (2003).

[57] R. Gao, Z. L. Wang, Z. Bai, W. A. de Heer, L. Dai, and M. Gao, Phys. Rev. Lett. **85**, 622 (2000).

[58] P. Poncharal, Z. L. Wang, D. Ugarte, and W. A. de Heer, Science **283**, 1513 (1999).

[59] S. T. Purcell, P. Vincent, C. Journet, and V. T. Binh, Phys. Rev. Lett. **89**, 276103 (2002).

[60] B. Reulet, A. Y. Kasumov, M. Kociak, R. Deblock, I. I. Khodos, Y. B. Gorbatov, V. T. Volkov, C. Journet, and H. Bouchiat, Phys. Rev. Lett. **85**, 2829 (2000).

[61] H. Jiang, M.-F. Yu, B. Liu, and Y. Huang, Phys. Rev. Lett. **93**, 185501 (2004).

[62] K. Jensen, C. Girit, W. Mickelson, and A. Zettl, Phys. Rev. Lett. **96**, 215503 (2006).

[63] T. Gabrielson, IEEE Trans. Electron Devices **40**, 903 (1993).

[64] T. R. Albrecht, P. Grutter, D. Horne, and D. Rugar, J. Appl. Phys. **69**, 668 (1991).

[65] A. N. Cleland and M. L. Roukes, J. Appl. Phys. **92**, 2758 (2002).

[66] L. Cutler and C. Searle, Proc. IEEE **54**, 136 (1966).

[67] Y. Yong and J. Vig, IEEE Trans. Ultrason. Ferroelectr. Freq. Control **36**, 452 (1989).

[68] J. Vig and Y. Kim, IEEE Trans. Ultrason. Ferroelectr. Freq. Control **46**, 1558 (1999).

[69] V. Bratman, M. Glyavin, T. Idehara, Y. Kalynov, A. Luchinin, V. Manuilov, S. Mitsudo, I. Ogawa, T. Saito, Y. Tatematsu, and V. Zapevalov, IEEE Trans. Plasma Sci. **37**, 36 (2009).

[70] D. J. M. Stothard, T. J. Edwards, D. Walsh, C. L. Thomson, C. F. Rae, M. H. Dunn, and P. G. Browne, Appl. Phys. Lett. **92**, 141105 (2008).

[71] I. M. Grace, S. W. Bailey, and C. J. Lambert, Phys. Rev. B **70**, 153405 (2004).

[72] R. Schoelkopf, P. Wahlgren, A. Kozhevnikov, P. Delsing, and D. Prober, Science **280**, 1238 (1998).

[73] R. G. Knobel and A. N. Cleland, Nature (London) **424**, 291 (2003).

[74] I. Bargatin, E. Myers, J. Arlett, B. Gudlewski, and M. Roukes, Appl. Phys. Lett. **86**, 133109 (2005).

[75] L. Sekaric, D. W. Carr, S. Evoy, J. M. Parpia, and H. G. Craighead, Sens. Actuators, A **101**, 215 (2002).